Measurements of 65 MeV Fe, Sn, and Pb$(n,n'x)$ continuum cross sections

E. L. Hjort,* F. P. Brady, J. R. Drummond, B. McEachern, J. H. Osborne, J. L. Romero, and D. S. Sorenson†
Crocker Nuclear Laboratory and Department of Physics, University of California, Davis, California 95616

H. H. K. Tang
IBM Microelectronics, Semiconductor Research and Development Center, East Fishkill Laboratory, Hopewell Junction, New York 12533
(Received 5 September 1995)

Inclusive inelastic scattering $(n,n'x)$ continuum cross sections have been measured at 65 MeV for Fe, Sn, and Pb targets using a detection system consisting of large area wire chambers and $\Delta E \cdot E$ scintillation detectors in conjunction with a CH_2 $n-p$ converter. The continuum $(n,n'x)$ spectra are compared with earlier $(p,p'x)$ data, and comparisons with cascade-statistical and preequilibrium continuum models are also made.

PACS number(s): 24.30.Cz, 25.40.Ep, 25.40.Fq, 21.60.−n

INTRODUCTION

In recent years a comprehensive investigation of giant resonance modes of nuclear excitation has been undertaken and considerable understanding has been developed [1,2]. Essential to this understanding are experimental results from a variety of probes [3]. Comparisons of results from different probes yield fundamental information about the dynamics of nuclear reactions and nuclear structure. Nucleon probes have played an important role. Examples are the discovery of isobaric analog states [4] via (p,nx) and of the giant quadrupole resonance in nuclei via inelastic proton $(p,p'x)$ scattering [5,6], the excitation of isovector giant resonances via (n,px) reactions [7], and of isobaric analog (Fermi) and Gamow-Teller states via (p,nx) [8–11] and (n,px) [12]. In many, if not all, hadronic-probe cases, the giant resonances are mingled with the excitation of a continuum from which one attempts to separate the resonance as a bump or bumps. (The history, or saga, of ''missing Gammow-Teller strength'' provides some indication of how difficult finding all the pieces can be.) Thus the measurements and understanding of the continuum region of inelastic and charge-exchange reactions are of fundamental importance. In addition, a knowledge of continuum cross sections is important in areas such as biomedical and material damage studies.

Several years ago we carried out and reported the first inelastic $(n,n'x)$ continuum measurements [13]. These were motivated by ^{118}Sn [14,15] and ^{208}Pb [16] $(\pi^{\pm},\pi^{\pm\prime}x)$ inelastic measurements at LAMPF whose analyses produced rather large ratios of neutron-to-proton matrix elements (Mn/Mp) for both GQR states and the continuum. Comparing our $(n,n'x)$ data to earlier Pb$(p,p'x)$ measurements [17] we concluded (in agreement with other analyses) that the continuum and GR inelastic nucleon cross section ratios are consistent with N/Z and not with those based on the inelastic pion analyses.

Here, we report new data from 65 MeV $(n,n'x)$ measurements for Fe and Sn targets. The continuum cross sections for these targets are compared to previous results from ^{120}Sn$(p,p'x)$ at 62 MeV [18] and ^{56}Fe$(p,p'x)$ at 61 MeV [19] and along with the Pb$(n,n'x)$ data are compared to continuum models. Besides the intrinsic interest in neutron-induced nuclear reactions, there is a wider interest in such nucleon cross-section measurements and models, and in being able to predict cross sections over a wide range of energies and nuclei. For example, there is a continuing interest in software and hardware failure in semiconductor devices due to neutron cosmic radiation.

EXPERIMENT AND RESULTS

As in the case of Pb$(n,n'x)$ [13], Sn and Fe$(n,n'x)$ spectra were measured using the neutron beam facility [20] and compact neutron detection system [21] located at Crocker Nuclear Laboratory at the University of California at Davis. The targets used were of natural isotopic content and were thin enough to limit multiple scattering to $\lesssim$10%. The neutron beam was produced by ^{7}Li$(p,n)^7$Be and in these experiments had a resolution of $\approx$1.1 MeV FWHM and a flux of $\approx 10^6$ neutrons/sec. The detection system (Fig. 1) utilizes multiwire proportional counters to track recoil protons which result from $n-p$ conversions of the scattered neutrons in a large-area CH_2 converter. One wire chamber placed in front of the CH_2 converter is used as a charged particle veto. The energy of a recoil proton is measured in a 15 cm×30 cm×2 cm thick NaI(Tl) crystal coupled to two 5″ photomultiplier tubes. Along with this E detector, a large area ΔE detector provides particle identification. Position dependent maps of the ΔE and E detectors' responses are used to improve their energy resolutions. For the E detector, δE (FWHM)$\leq$1 MeV over most sections of the detector area. The energy of the scattered neutron is calculated from the proton's energy and from the angle of the $n-p$ conversion. The overall measured energy resolution of the system (2.7

*Present address: Physics Dept., Purdue University, West Lafayette, IN 47907.
†Present address: P15, Los Alamos National Laboratory, Los Alamos, NM 87545.

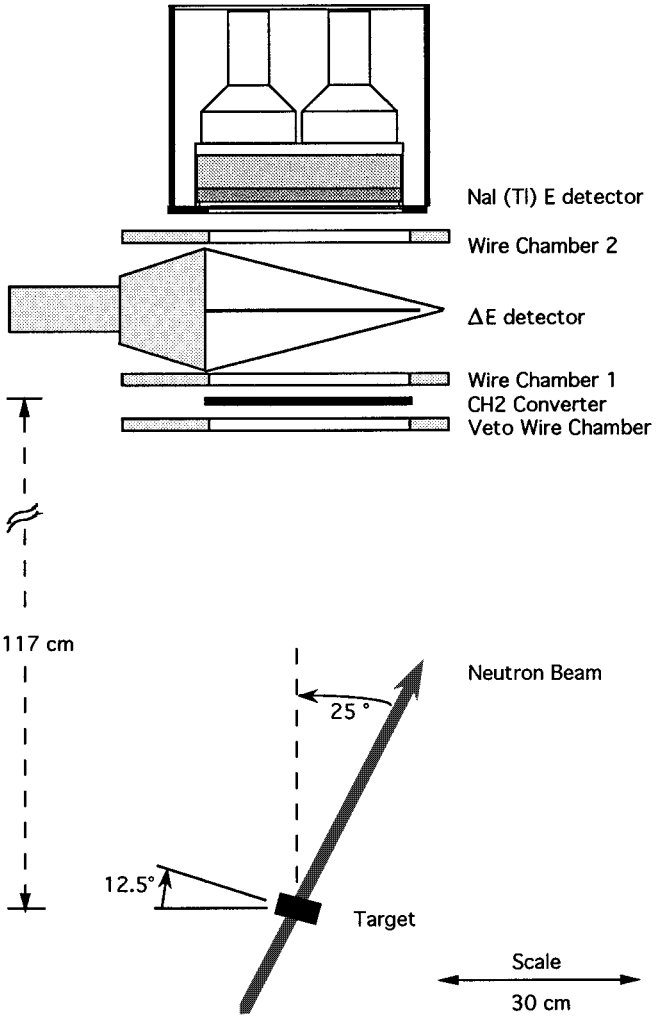

FIG. 1. Schematic of the $(n,n'x)$ detection system.

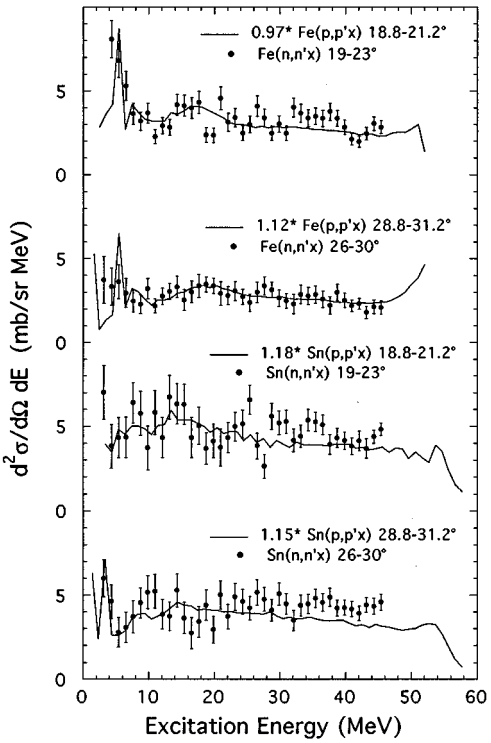

FIG. 2. 65 MeV $(n,n'x)$ spectra (data points) for Fe and Sn compared to $(p,p'x)$ spectra (continuous lines) at similar energies.

MeV FWHM) results from approximately equal contributions due to uncertainties in the neutron beam energy, energy losses, and their fluctuations in the CH_2 converter, the resolution of the NaI(Tl) detector and uncertainties in the proton's recoil angle due primarily to the size of the beam on the target ($\simeq 2.5\times 2.5$ cm^2). The predicted resolution (2.3 MeV FWHM) is probably not reached due largely to the systematic uncertainties in the E detector response map.

For continuum measurements (as distinct from elastic) a complication arises due to events from $^{12}C(n,p)$ reactions in the CH_2 converter, Because $Q=-12.6$ MeV for this reaction, elastically scattered neutrons which are converted by carbon will incorrectly appear to have the same energy as lower-energy, inelastically scattered neutrons converted by hydrogen. Thus events from these two reactions in the converter (which produce similar proton energies) result from scattered neutrons of different energies. By increasing the distance from the target to the CH_2 converter the undesired $^{12}C(n,p)$ events can be separated over much of the overlap range from the $^1H(n,p)$ events by their neutron time-of-flight (TOF) difference. In practice the separation is not perfect, so data were taken with CH_2 and C converters with the target both in and out and a background subtraction was performed. The Binstock parametrization [22] of the $n-p$ cross section (adjusted slightly [23] to allow for more recent $n-p$ data [24]) was used to correct for the energy dependence of the converter's efficiency. Final spectra were obtained by normalizing the continuum to the elastic peak. The elastic cross section was measured using the same system [21], with fits to elastic $^1H(n,n)^1H$ data [24] providing an absolute normalization. Target-out backgrounds due mainly to neutron-air interactions were small and subtracted out after proper normalization.

Figure 2 shows the 65 MeV Fe and Sn$(n,n'x)$ and similar energy $(p,p'x)$ spectra. The error bars reflect statistical as well as systematic errors, and become smaller at lower energies because the TOF elimination of carbon conversion events is cleaner. The angular range was chosen to be that where the isoscalar quadrupole is the dominant giant resonance. However, statistical uncertainties preclude a separa-

TABLE I. The experimental values of the cross section ratios for $10\leqslant E_x\leqslant 25$ MeV.

	Fe		Sn		Pb[a]	
$R_{\rm exp}=\dfrac{\sigma(n,n')}{\sigma(p,p')}$	20°	30°	20°	30°	20°	28°
	0.97 ± 0.12	1.12 ± 1.16	1.18 ± 0.15	1.15 ± 0.16	1.50 ± 0.22	1.27 ± 0.21

[a]Data from [13]

tion of the GQR from the continuum background. The off-scale elastic peak (not shown) would be at zero excitation energy, and the cutoff in the data at about 45 MeV excitation is due to the low-energy limit of the detection system. The solid lines show the 62 MeV ^{120}Sn$(p,p'x)$ data [18] and the 61 MeV ^{56}Fe$(p,p'x)$ data [19], multiplied by appropriate factors such that the integrated cross sections from excitation energies of 10–25 MeV are equal to those of the neutron data. These factors, and those for Pb, and the corresponding mean lab angles, are given in Table I.

Continuum model comparisons

In this energy range, pioneering measurements and studies of $(p,p'x)$ energy and angle spectra were carried out at ORNL by Bertrand and Peele [25]. The authors [25] mostly compare their measurements to predictions from a version of the intranuclear cascade model due to Bertini [26]. At the time, the importance of such comparisons was due to the fact that the validity of the cascade model was not expected to extend below $\cong$150 MeV incident nucleon energy. However, except for the most forward angles, where a predicted quasi-elastic peak is not seen in the data, the cascade model predictions agree quite well with the 60 MeV ORNL data. When nuclear mean-field distortion effects are included in the model, this peak is much reduced and spread into the lower-energy continuum [25].

Another model, which has been extensively used, is the preequilibrium statistical model initially proposed by Griffin [27] and developed by Blann [28] and others. In this model, excitation of the nucleus is described by the successive excitation of excitons or particle-hole pairs. Kalbach and Mann [29] have extended their preequilibrium model, PRECO, which is based on the exciton model, to obtain PRECO-D [30] which can predict angular distributions. They are guided by physical principles, but in the end the model is largely phenomenological, and based on a wide range of experimental data.

A detailed quantum-mechanical theory of preequilibrium reactions has been given by Feshbach, Kerman, and Koonin [31], who divide the reaction cross section into two parts. One, called (statistical) multistep direct (MSD), exhibits forward angle peaking. The other, (statistical) multistep compound (MSC), is 90° cm symmetric. These basis ideas of MSD and MSC are utilized by Kalbach and Mann [29] in their phenomonological study on which PRECO-D is based. Figure 3 shows comparisons of the predictions of this model with the Fe and Sn$(n,n'x)$ data. The model does not attempt to account for low-lying states or resonances (or for the elastic tail one sees extending down in energy). We did not adjust any parameters. Except at the low excitations, fairly good general agreement with the data is found.

In Fig. 4 the continuum data are compared to predictions of the cascade-statistical (CS) model of Tang *et al.* [32]. This model assumes two stages. The initial (intranuclear cascade) stage uses a modified version of Bertini's MECC-7 code [26]. This simulated a sequence of quasifree nucleon-nucleon collisions which incorporate the effects of the Fermi motion of target nucleons and of the Pauli principle. The second stage is the statistical decay of an excited compound nucleus in a model developed by the authors [32], which predicts rather well low-energy particle spectra, and which includes heavier fragments as would be produced in higher energy fragmentation of O, Si, and heavier nuclei. Our measurements test the model predictions of the first stage. As we do not measure the low-energy emission, the statistical decay predictions are not tested. This model predicts absolute cross sections, and no parameter adjustments are used to fit the data. It can be seen in Figs. 4(a)–(c) that the agreement with the data is reasonable, although not within experimental uncertainties in some energies ranges for each target nucleus.

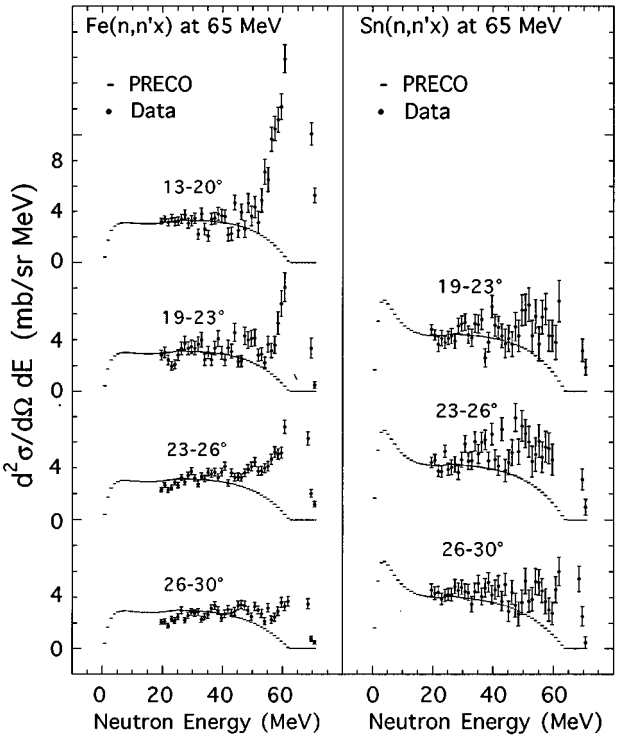

FIG. 3. Comparison of the predictions of PRECO-D with the $(n,n'x)$ data. Absolute model and measured cross sections are plotted vs neutron (c.m.) energy. For clarity, part of the elastic peak has been suppressed.

It is interesting to compare the CS model to data at these energies, because they are at the lower end of the energy range of model validity. The model does not contain a nuclear mean field which is well known to be important at these energies. It attempts to incorporate approximately mean-field effects through the use of the true effective interaction in the nuclear medium. As noted above, besides a realistic interaction, Pauli blocking and Fermi motion of the target nucleons is incorporated into the Monte Carlo sampling procedure.

In Fig. 5 comparison of the CS model with both $(p,p'x)$ [17–19] and $(n,n'x)$ is made. The model predicts the essential features of the data. For all the experimental spectra the $(n,n'x)$ cross sections are, in general, higher than the $(p,p'x)$ and the differences increase with $N-Z$. This may, at first, seem puzzling since the targets contain more neutrons than protons, and the interaction between unlike nucleons, V_{np}, dominates. However, in macroscopic DW calculations we find that the larger mean-field distortions for protons, due to the Coulomb and $(N-Z)/A$ optical potential terms, reduce the $(p,p'x)$ cross sections relative to the $(n,n'x)$, more than

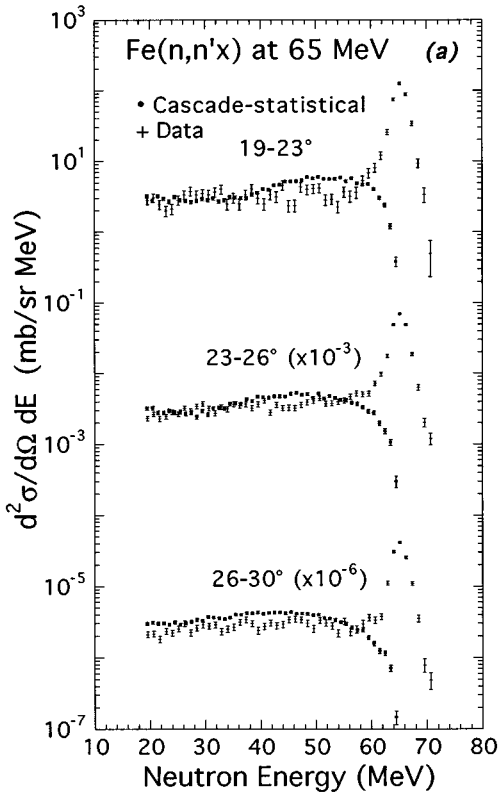

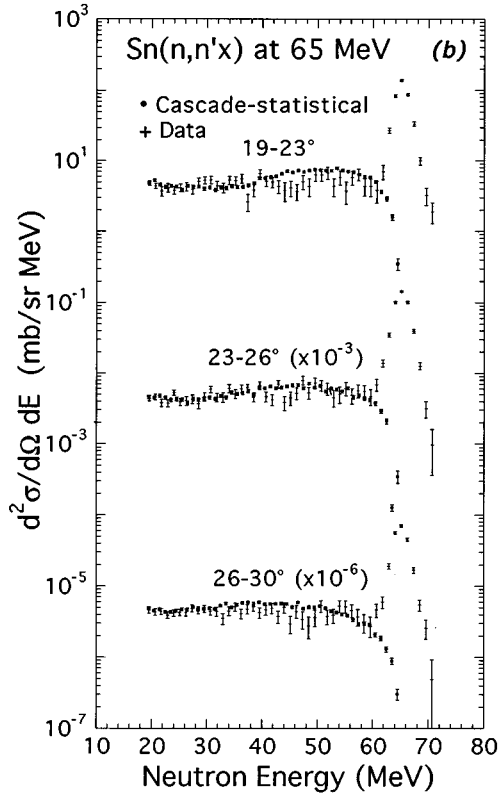

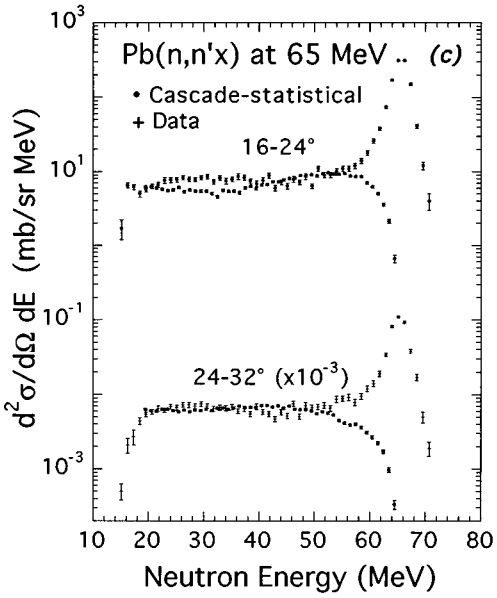

FIG. 4. Comparisons of the predictions of the cascade statistical model with the 65 MeV $(n,n'x)$ data for (a) Fe, (b) Sn, and (c) Pb. Absolute, angle-averaged, model and measured cross sections are plotted vs neutron (c.m.) energy. The model does not include elastic scattering or explicitly inelastic scattering to low-lying states.

compensating the (N/Z) ratio of target neutrons to protons. In the spirit of the macroscopic model, the experimental $(p,p'x)/(n,n'x)$ continuum cross-section ratios are reproduced by a simple single-step inelastic–quasielastic scattering model with the DW amplitude having terms of the form [33] $\int dq\ q^2 D(q,E_p)t(q,E_p)\rho(q,E_x)$, where (in q space) D is the distortion factor, ρ is the nucleon density $(\rho_n/\rho_p = N/Z)$ and t represents the effective nucleon-nucleon interaction. (E_p is the projectile KE.)

In the CS predictions (Fig. 5) one sees at the more forward angles a broad hump above the data at lower excitations. This must be due to quasielastic scattering. The CS model has no mean-field distortion effects which would tend to spread in angle and energy the effects of such scattering.

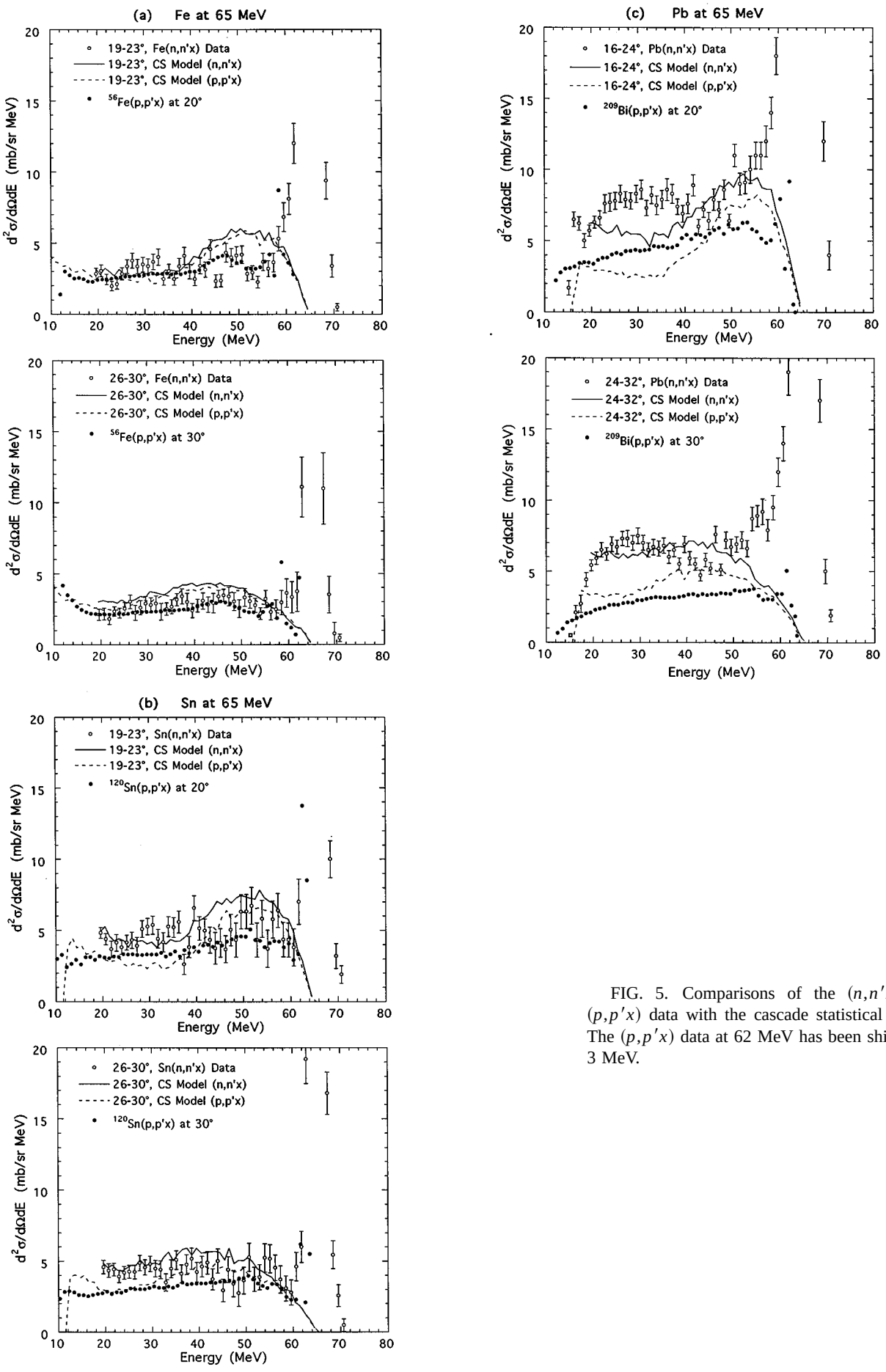

FIG. 5. Comparisons of the ($n,n'x$) and ($p,p'x$) data with the cascade statistical model. The ($p,p'x$) data at 62 MeV has been shifted by 3 MeV.

(As noted above, the CS model attempts to include these distortion effects via the in-medium nucleon-nucleon interaction.)

We conclude that, in general, continuum models describe the $(n,n'x)$ spectra at these energies to within about 25%, and that the differences between measured $(p,p'x)$ and $(n,n'x)$ spectra can be understood intuitively within the framework of inelastic scattering models. It appears that the CS model effective interactions do not completely simulate mean-field distortion effects.

The support of the National Science Foundation (Grant Nos. PHY87-22008 and PHY90-24794), and the Associated Western Universities is gratefully acknowledged along with the support and assistance provided by the Department of Physics and Crocker Nuclear Laboratory and their staff.

[1] J. Speth and A. van der Woude, Rep. Prog. Phys. **44**, 719 (1981).
[2] *Spin Excitation in Nuclei*, edited by F. Petrovich *et al.* (Plenum, New York, 1984).
[3] F. Petrovich, J. A. Carr, and H. McManus, Annu. Rev. Nucl. Part. Sci. **36**, 29 (1986).
[4] For early (p,n) data and references on Fermi transitions see the conference proceedings, *Isobaric Spin in Nuclear Physics*, edited by John D. Fox and Donald Robson (Academic Press, New York, 1966).
[5] M. B. Lewis and F. E. Bertrand, Nucl. Phys. **A196**, 337 (1972).
[6] F. E. Bertrand, Annu. Rev. Nucl. Sci. **26**, 468 (1976).
[7] F. P. Brady, N. S. P. King, M. W. McNaughton, and G. R. Satchler, Phys. Rev. Lett. **36**, 15 (1976). Even earlier, D. F. Measday and J. N. Palmieri, Phys. Rev. **161**, 1071 (1967) were able with only 6 MeV resolution to observe analog resonances via (n,p). F. P. Brady and G. A. Needham, in *The (p,n) Reaction and the Nucleon-Nucleon Force* [9], p. 357, and N. S. P. King and J. L. Ullmann, in *ibid.*, p. 372 provide a review of early U. C. Davis data.
[8] R. R. Doering, Aaron Galonsky, D. M. Patterson, and G. F. Bertsch, Phys. Rev. Lett. **35**, 1891 (1975).
[9] C. D. Goodman, in *The (p,n) Reaction and the Nucleon-Nucleon Force*, edited by C. D. Goodman, S. M. Austin, S. D. Bloom, J. Rapaport, and G. R. Satchler (Plenum Press, New York, 1980), p. 149, and references cited therein.
[10] D. E. Bainum *et al.*, Phys. Rev. Lett. **44**, 1751 (1980).
[11] C. D. Goodman *et al.*, Phys. Rev. Lett. **44**, 1755 (1980).
[12] F. P. Brady, C. M. Castaneda, G. A. Needham, J. L. Ullmann, J. L. Romero, T. D. Ford, M. L. Johnson, N. S. P. King, C. M. Morris, F. Petrovich, and R. H. Howell, Phys. Rev. Lett. **48**, 860 (1982).
[13] E. L. Hjort, F. P. Brady, J. L. Romero, J. R. Drummond, M. A. Hamilton, B. McEachern, R. D. Smith, V. R. Brown, F. Petrovich, and V. A. Madsen, Phys. Rev. Lett. **62**, 870 (1989).
[14] J. L. Ullmann, J. J. Kraushaar, T. G. Peterson, R. S. Raymond, R. A. Ristinen, N. S. P. King, R. L. Boudrie, C. L. Morris, R. E. Anderson, and E. R. Siciliano, Phys. Rev. C **31**, 177 (1985).
[15] J. L. Ullmann *et al.*, Phys. Rev. Lett. **51**, 1038 (1983).
[16] S. J. Seestrom-Morris, C. L. Morris, J. M. Moss, T. A. Carey, D. Drake, J.-C. Dousse, L. C. Bland, and G. S. Adams, Phys. Rev. C **33**, 1847 (1986).
[17] M. B. Lewis, F. E. Bertrand, and D. J. Horen, Phys. Rev. C **8**, 298 (1973). There are more recent and similar data at 61 MeV in F. E. Bertrand and D. C. Kocker, *ibid.* **13**, 2241 (1976).
[18] F. E. Bertrand and R. W. Peele, Oak Ridge National Laboratory Report No. ORNL-4471, 1970.
[19] F. E. Bertrand and R. W. Peele, Oak Ridge National Laboratory Report No. ORNL-4456, 1970.
[20] F. P. Brady, in *A Probe of Nuclear Structure*, edited by J. Rapaport, R. W. Finlay, S. M. Grimes, and F. S. Dietrich, AIP Conf. Proc. No. 124 (AIP, New York, 1985), p. 171.
[21] F. P. Brady, T. D. Ford, G. A. Needham, J. L. Romero, C. M. Castaneda and M. L. Webb, Nucl. Instrum. Methods **228**, 89 (1984).
[22] J. Binstock, Phys. Rev. C **10**, 19 (1974).
[23] E. L. Hjort, Ph.D. dissertation, U. C. Davis, 1990 (unpublished).
[24] R. A. Arndt and B. J. ver West, in *Proceedings of the 9th International Conference on the Few Body Problem*, Eugene, Oregon, edited by M. J. Moravcsik (University of Oregon, Oregon, 1980), Vol. 1, p. VIII-3, and the SAID program which can be reached and used via the Internet.
[25] F. E. Bertrand and R. W. Peele, Phys. Rev. C **8**, 1045 (1973). This paper also provides references to the ORNL reports containing the data.
[26] H. W. Bertini, Phys. Rev. **131**, 1801 (1963); **138**, B2 (1965); **188**, 1711 (1969).
[27] J. J. Griffin, Phys. Rev. Lett. **17**, 478 (1966).
[28] M. Blann, Phys. Rev. Lett. **21**, 1357 (1968).
[29] C. Kalbach and F. Mann, Phys. Rev. C **23**, 112 (1981); C. Kalbach, *ibid.* **23**, 124 (1981).
[30] PRECO-D, available from C. Kalbach.
[31] H. Feshbach, A. Kerman, and S. Koonin, Ann. Phys. (N.Y.) **125**, 429 (1980).
[32] H. H. K. Tang, G. R. Srinivasan, and N. Azziz, Phys. Rev. C **42**, 1598 (1990).
[33] F. Petrovich, Nucl. Phys. **A 251**, 143 (1975).